



Identification of Key microRNAs in Diabetes Mellitus Erectile Dysfunction Rats with Stem Cell Therapy by Bioinformatic Analysis of Deep Sequencing Data

Jiaqi Kang^{1,*}, Yuxuan Song^{2,3,*}, Zhixin Zhang¹, Shangren Wang¹, Yi Lu¹, Xiaoqiang Liu¹

¹Department of Urology, Tianjin Medical University General Hospital, Tianjin, ²Department of Urology, Peking University People's Hospital, ³Biomedical Pioneering Innovation Center (BIOPIC), School of Life Sciences, Peking University, Beijing, China

Purpose: Diabetes mellitus erectile dysfunction (DMED) is a common resulting complication of diabetes. Studies have shown mesenchymal stem cell (MSC)-based therapy was beneficial in alleviating erectile function of DMED rats. While the pathogenesis of DMED and the mechanism MSCs actions are unclear.

Materials and Methods: We constructed a rat model of DMED with or without intracavernous injection of MSCs, and performed microRNA (miRNA) sequencing of corpora cavernosa tissues.

Results: We identified three overlapping differentially expressed miRNAs (rno-miR-1298, rno-miR-122-5p, and rno-miR-6321) of the normal control group, DMED group, and DMED+MSCs group. We predicted 285 target genes of three miRNAs through RNAhybrid and miRanda database and constructed a miRNA-target gene network through Cytoscape. Next, we constructed protein-protein interaction networks through STRING database and identified the top 10 hub genes with highest connectivity scores. Five GO terms including cellular response to growth factor stimulus (GO:0071363), ossification (GO:0001503), response to steroid hormone (GO:0048545), angiogenesis (GO:0001525), positive regulation of apoptotic process (GO:0043065), and one Reactome pathway (Innate Immune System) were significantly enriched by 10 hub genes using the Metascape database. We selected the GSE2457 dataset to validate the expression of hub genes and found only the expression of B4galt1 was statistically different ($p < 0.001$). B4galt1 was highly expressed in penile tissues of diabetic rats and would be negatively regulated by rno-miR-1298.

Conclusions: Three key miRNAs were identified in DMED rats with stem cell therapy and the miR-1298/B4GalT1 axis might exert function in stem cell therapy for ED.

Keywords: Diabetes mellitus; Erectile dysfunction; Mesenchymal stem cells; MicroRNAs

This is an Open Access article distributed under the terms of the Creative Commons Attribution Non-Commercial License (<http://creativecommons.org/licenses/by-nc/4.0>) which permits unrestricted non-commercial use, distribution, and reproduction in any medium, provided the original work is properly cited.

Received: Aug 6, 2021 **Revised:** Sep 16, 2021 **Accepted:** Sep 30, 2021 **Published online** Jan 2, 2022

Correspondence to: Xiaoqiang Liu <https://orcid.org/0000-0003-3524-6783>

Department of Urology, Tianjin Medical University General Hospital, No. 154, Anshan Road, Heping District, Tianjin 300052, China.

Tel: +86-17732531049, **Fax:** +86-60361614, **E-mail:** xiaoqiangliu1@163.com

*These authors contributed equally to this work as co-first authors.

INTRODUCTION

Erectile dysfunction (ED), also referred to as “impotence”, is defined as the inability to achieve and maintain an erection sufficient for acquiring satisfactory sexual performance [1]. More than 50% of men over 40-year-old suffer from ED [2]. It has been proved that ED harms the quality of life and psychosocial health of patients and their partners [3,4]. Diabetes mellitus (DM) is recognized as an important risk factor that may cause ED. Similarly, ED affects nearly half of men who suffered from diabetes [5]. Among diabetics, ED tends to occur 10 to 15 years earlier and is more serious, associated with poor response to treatment compared with non-diabetic patients [6]. Therefore, the study on diabetes mellitus erectile function (DMED) should be given enough attention.

Although phosphodiesterase type 5 inhibitors is currently recommended as first-line treatment of ED, they cannot correct the underlying penile pathophysiology, such as vascular endothelial dysfunction secondary to DM, that is responsible for the ED [7]. As a novel method, stem cell therapy has been widely concerned for its potential in DMED treatment [8]. So far, multiple stem cells, including adipose tissue-derived stem cells [9], mesenchymal stem cells (MSCs) [10,11], embryonic stem cells [12], and urine-derived stem cells [13], were shown to be an effective strategy for DMED in rat models. With a variety of sources covering umbilical cord blood, adipose tissue, and bone marrow [14], MSCs are recognized as an ideal candidate for the treatment of DMED due to their positive therapeutic effects in different types of ED [15,16]. Nevertheless, stem cell therapy for ED is still in the exploratory stage of development, and the mechanisms by which MSCs contribute to DMED are still not fully clarified.

MicroRNA (miRNA), a category of small non-coding RNA with 19 to 25 nucleotides, was initially identified in 1993 [17]. Increasing number of studies have shown that miRNAs participate in the development of many diseases such as cancer, cardiovascular events, and ED [18,19]. Wen et al [20] found that miR-205 contributed to the pathogenesis of DMED *via* down-regulating androgen receptor expression. Thus, miR-205 might be a potential therapeutic target of DMED. On the other hand, miRNAs are involved in regulating the self-renewal and pluripotency of stem cells. Liu et al [16] reported that miRNA-145 engineered MSCs effectively

alleviated age-related ED, and transplantation of miR-145-overexpressing MSCs would become a promising novel method for age-related ED therapy. Namely, miRNAs serve key roles in the pathogenesis and treatment of ED.

As far as we know, there were few studies currently on the miRNA expression profiles of penis tissues in DMED treated with MSCs. The present study was performed to identify differentially expressed miRNAs (DEMs) in corpora cavernosa tissues of DMED rats and analyze target genes and signaling pathways regulated by DEMs, to explore the mechanism by which stem cells exert their actions.

MATERIALS AND METHODS

1. Animal experiment

1) Animal procedures

All rats were male Sprague-Dawley rats aged 8 weeks purchased from Beijing HFK Bioscience Co., Ltd (Beijing, China), with normal erectile function verified by mating tests. Rats were randomly selected into three groups, including normal control (NC), DEMD, and DMED+MSCs groups (ten rats per group, five rats per cage). The DMED group and the DMED+MSCs group were fed a high-fat diet, but rats in the NC group were fed a normal diet. Following eight weeks of dietary intervention, the DMED group and the DMED+MSCs group were intraperitoneally injected with a single dose of 30 mg/kg streptozotocin (Sigma, St. Louis, MO, USA). The NC group was injected with an equal volume of 0.1 mol/L citrate buffer without streptozotocin. Blood glucose concentrations were monitored three days after injection and rats were regarded as diabetic when the fasting blood glucose level was above 16.7 mmol/L. Eight weeks after streptozotocin injection, Apomorphine (100 mg/kg) was employed to identify the ED rats based on the protocol of Heaton et al's study [21]. Rats that developed ED in the DMED+MSCs group were injected with 100 μ L phosphate-buffered saline (PBS) containing 1×10^6 human umbilical cord-derived MSCs (hUC-MSCs) into the corpus cavernosum, and rats in the DMED group were injected with 100 μ L PBS alone. Unicell Life Technology Co., Ltd (Tianjin, China) provided hUC-MSCs for the study.

2) Ethics statement

The procedures used and the care of animals were approved by Experimental Animal Ethics and Welfare Committee of Tianjin Medical University General Hospital (approval No.IRB2021-DWFL-099).

2. Erectile function evaluation

Four weeks after stem cell treatment, erectile function was measured by electric stimulation of the cavernous nerve as previously reported [22]. The stimulus parameters were 5v, 15Hz, 5ms width, and a duration of 1 minute. The pressure was recorded and analyzed by the Medlab software (Nanjing, China). The erectile function was presented as the max intracavernous pressure (ICP) and the ratio of ICP/main arterial pressure (ICP/MAP) to avoid the influence of blood pressure variations.

3. RNA extraction, library preparation, and sequencing

Total RNA was isolated and purified using TRIzol reagent (Invitrogen, Carlsbad, CA, USA) following the manufacturer's procedure. The RNA amount and purity of each sample were quantified using NanoDrop 2000 (Thermo Fisher Scientific, Waltham, MA, USA). Approximately 5 µg of total RNA was used to deplete ribosomal RNA according to the manuscript of the Ribo-Zero™ rRNA Removal Kit (Illumina, San Diego, CA, USA). Sequencing libraries were generated using the TruSeq RNA Sample Preparation Kit (Illumina). After that, we performed RT-PCR with Phusion High-Fidelity DNA polymerase, Index (X) Primer, and Universal PCR primers. Ultimately, we purified the products using the AMPure XP system (Beckman Coulter, Indianapolis, IN, USA) and evaluated library quality by Agilent 2100 bioanalyzer (Agilent Technologies, Santa Clara, CA, USA). After purification and enrichment, the sequencing library was then sequenced on Illumina HiSeq 2500 platform (Illumina) by GENESKY Biotechnologies Inc. (Shanghai, China).

4. Processing of sequencing data

We assessed read quality using FastQC v0.10 software (<https://www.bioinformatics.babraham.ac.uk/projects/fastqc/>). Low-quality reads and adaptor sequences were trimmed out through Trim Galore (https://www.bioinformatics.babraham.ac.uk/projects/trim_galore/). Then, we mapped clean reads to the hg19 reference

genome by Bowtie v1.1.2 to identify small RNA loci including miRNAs. After that, the known mature miRNA expression profile was generated using the miRDeep2 package (<https://github.com/rajewsky-lab/mirdeep2>). Normalized reads were generated by the trimmed mean of M-values normalization. Counts for each miRNA were calculated by Reads Per Kilobase per Million mapped reads (RPKM). The processing of sequencing data was performed by GENESKY Biotechnologies Inc.

5. Identification of differentially expressed miRNAs

The edgeR package was applied to identify the DEMs with the standard of $|\log(\text{fold change})| > 1$ and adjusted p-value < 0.05 [23]. We analyzed and generated DEMs by the comparisons between the DMED *versus* NC and DMED *versus* DMED+MSCs. Volcano plots and heatmaps were visualized with pheatmap and ggplot2 packages in R software. Subsequently, Venny2.1 (<https://bioinfogp.cnb.csic.es/tools/venny/index.html>), one online tool, was employed to select overlapping dysregulated DEMs of the two comparisons.

6. Construction of the miRNA-target gene network

The bioinformatics databases including RNAhybrid (<http://bibiserv.techfak.uni-bielefeld.de/rnahybrid/>) [24] and miRanda (<http://www.microrna.org>) [25] were applied for target gene prediction of the overlapping DEMs. Only genes that were predicted by both tools were considered target genes of those DEMs. The miRNA-target gene network was visualized by Cytoscape v3.7.1 software [26].

7. Construction of protein-protein interaction network

Based on the target genes predicted, the protein-protein interaction (PPI) network was constructed through the Search Tool for the Retrieval of Interacting Genes (STRING) database [27] and the visualization was performed by Cytoscape v3.7.1. The cytoHubba plug-in was used to rank target genes and the MCODE plug-in was used to identify the significant modules (degree threshold: 2, k-core threshold: 2).

8. Functional enrichment analysis

To explain the biological processes (BPs) of target

genes, we performed Gene Ontology (GO) including BP, molecular function (MF), and cellular component (CC), and Kyoto Encyclopedia of Genes and Genomes (KEGG) enrichment analysis by the R package clusterProfiler (version 3.18.1) [28]. Metascape (<https://metascape.org/gp/index.html>) [29] was applied to performed functional enrichment analysis of top 10 hub genes. Terms with a p-value <0.05 were recognized as statistically significant.

9. Validation of hub genes by GEO dataset

We downloaded the GSE2457 dataset from the Gene Expression Omnibus (GEO) repository (<https://www.ncbi.nlm.nih.gov/geo/>) to validate the expression of hub genes. The dataset compared the gene expression profile of penile tissues in diabetic and control rats based on the platform of GPL341 (Affymetrix Rat Expression 230A Array), in which 5 diabetic and 5 control tissues were selected [30]. Normalized expression data were log-transformed before analysis.

10. Statistical analysis

Quantitative data in this study were presented as mean±standard deviation. One-way ANOVA test was performed to make inter-group comparisons of parametric data. Comparisons of nonparametric data were performed through the Kruskal–Wallis test. We adopted GraphPad Prism 8.0 (GraphPad Software Inc., San Diego, CA, USA) to perform statistical analysis. Differences of p-value <0.05 were considered statistically significant and all statistical tests were two-tailed.

RESULTS

The study flow chart was illustrated in Fig. 1. Basic parameters of rats such as body weight, fasting plasma glucose, and erectile function for each group were summarized in Table 1. The mean bodyweight of the DMED group was significantly lower than NC group ($p<0.05$), blood glucose was higher than that of the NC group ($p<0.05$), and Max ICP ($p<0.05$) and ICP/MAP ($p<0.05$) were significantly lower than NC group, which proved that the DMED rat model was successfully constructed. After stem cell therapy, the Max ICP ($p<0.05$) and ICP/MAP ($p<0.05$) of the DMED+MSCs group were significantly higher than the DMED group, but there was no significant change in body weight and fasting glucose. Representative images of MAP and ICP were

shown in Fig. 2A, 2B.

1. Identification of DEMs

A total of 20 DEMs were screened in the comparison of the DMED group and the NC group, including 5 downregulated miRNAs and 15 upregulated miRNAs (Fig. 3A, 3C). Among the comparison of the DMED group and DMED+MSCs group, we identified 24 DEMs including 20 downregulated miRNAs and 4 upregulated miRNAs (Fig. 3B, 3D). The Venn analysis showed that three DEMs were overlapped among the two comparisons (Fig. 3E, 3F). Specifically, rno-miR-1298 was down-regulated, while rno-miR-122-5p and rno-miR-6321 were up-regulated in DMED rat samples (Table 2).

2. The regulatory network of miRNA-mRNA

To better understand the downstream regulatory mechanism of DEMs, we predicted latent target genes of three overlapped miRNAs by making use of RNA-hybrid and miRanda. We predicted 88 rno-miR-1298 target genes, 99 rno-miR-122-5p target genes, and 98 rno-miR-6321 target gene respectively. We displayed the miRNA-gene network in Fig. 4.

3. Functional enrichment analysis of target genes

To get a better insight into the biological function of DEMs, we performed GO and KEGG enrichment analysis on the 285 target genes of DEMs. As shown in Fig. 5A-5C, CC terms were mainly enriched in histone deacetylase complex, sarcoplasmic reticulum, and integral component of mitochondrial outer membrane. BP analysis showed that target genes were enriched in response to cycloheximide, retrograde transport, endosome to Golgi, and activation of GTPase activity. MF terms including galactosyltransferase activity, UDP-galactosyltransferase activity, and enzyme activator activity were enriched significantly. The KEGG pathway analysis revealed that target genes were particularly enriched in pathways of glycosphingolipid biosynthesis-lacto and neolacto series, necroptosis, and GnRH signaling pathway (Fig. 5D).

4. Construction of PPI network and identification of hub genes

As shown in Fig. 6, we constructed a PPI network to display the interaction of 285 target genes through the STRING database. Next, the top 10 hub genes with

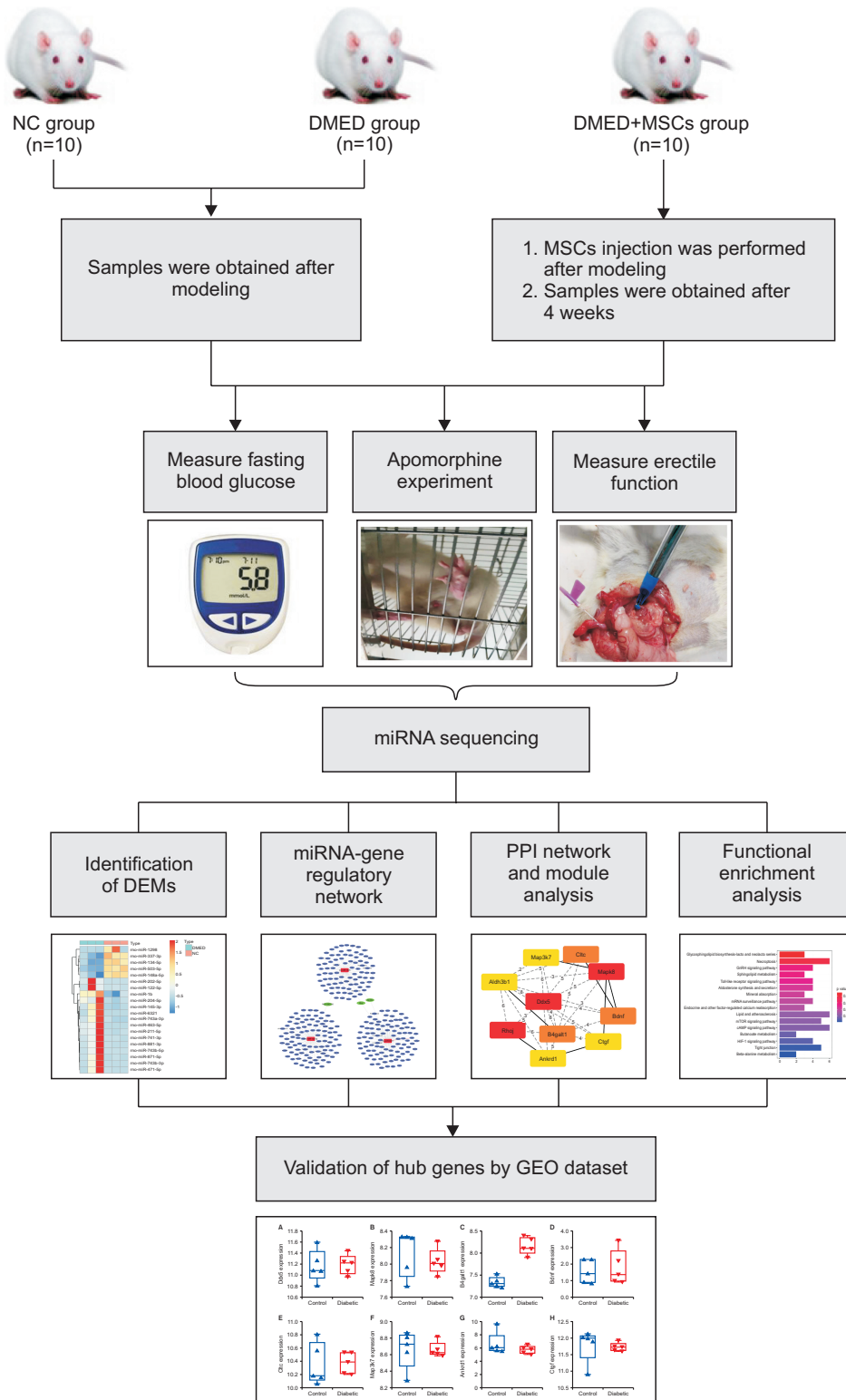


Fig. 1. Workflow of the study. NC: normal control, DMED: diabetes mellitus erectile dysfunction, MSC: mesenchymal stem cell, DEM: differentially expressed miRNA, PPI: protein-protein interaction, GEO: Gene Expression Omnibus.

the highest connectivity degree in the PPI network were identified through the cytoHubba, which were displayed in Fig. 7A and Table 3. Furthermore, we performed module analysis by the MCODE plugin and generated six clusters displayed in Fig. 7B.

5. Functional enrichment analysis of hub genes

Metascape was applied to perform enrichment analysis of 10 hub genes. As a result in Fig. 7C, 7D, we identified that five GO terms including cellular response to growth

Table 1. Basic parameters and erectile function of rats

Group	NC	DMED	DMED+MSCs
Body weight (g)	444.3±33.0	256.0±29.1 ^a	239.4±17.4 ^a
Glucose levels (mmol/L)	5.29±0.70	24.9±4.3 ^a	26.7±2.5 ^a
Max ICP (mmHg)	81.2±3.67	47.60±2.39 ^a	71.66±2.34 ^b
MAP (mmHg)	120.35±10.30	110.24±9.35	109.29±9.86
ICP/MAP	0.67±0.03	0.43±0.02 ^a	0.66±0.02 ^b

The level of MAP, ICP, and ICP/MAP was measurement data, which was expressed as mean±SD.

NC: normal control, DMED: diabetes mellitus erectile dysfunction, MSC: mesenchymal stem cell, ICP: intracavernous pressure, MAP: main arterial pressure.

^ap<0.05 versus NC group. ^bp<0.05 versus DMED group.

Data in each group were analyzed with oneway ANOVA.

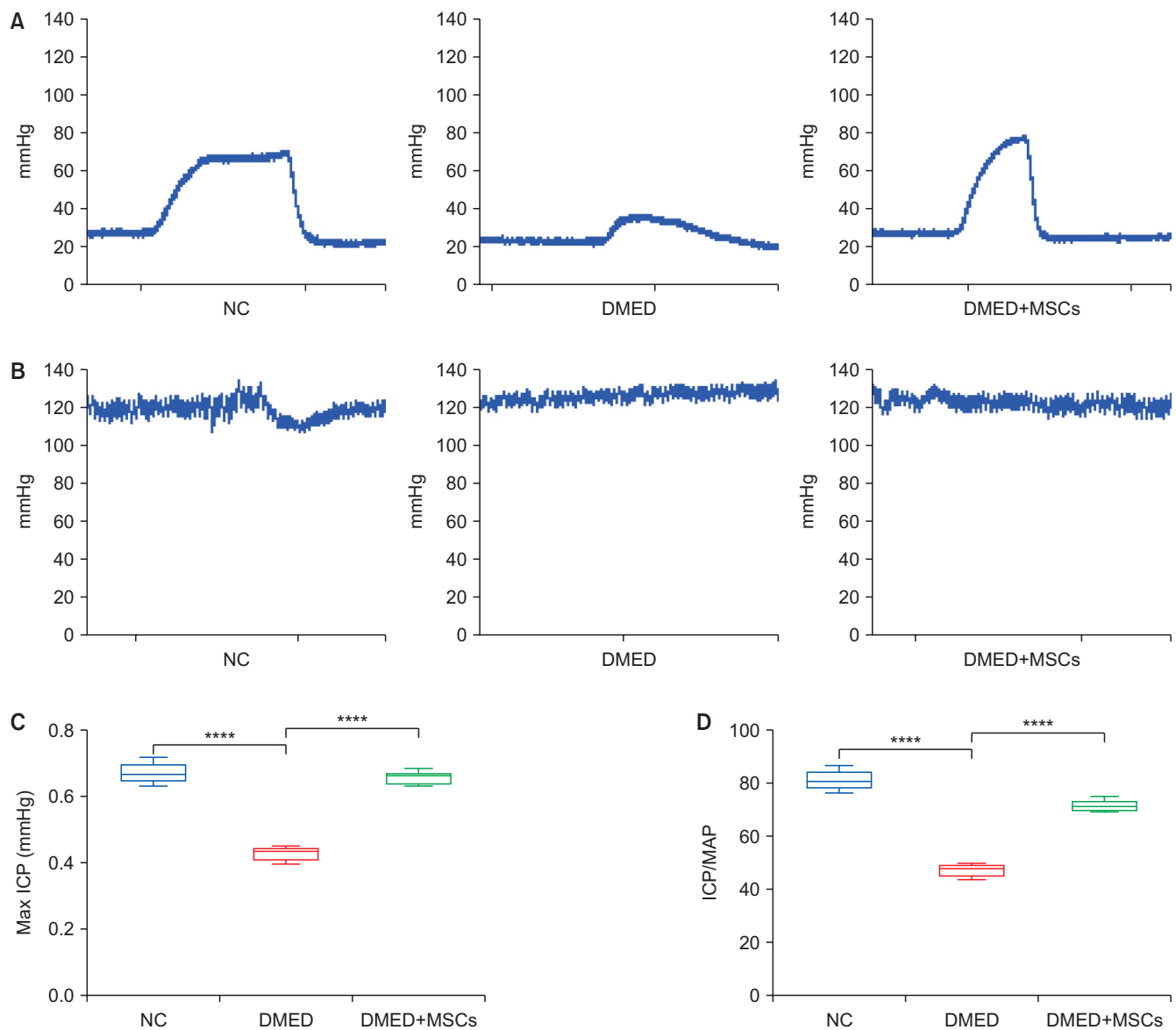


Fig. 2. The erectile function of rats. (A) ICP. (B) MAP. (C) Max ICP. (D) ICP/MAP. NC: normal control, DMED: diabetes mellitus erectile dysfunction, MSC: mesenchymal stem cell, ICP: intracavernous pressure, MAP: main arterial pressure. ****p<0.0001.

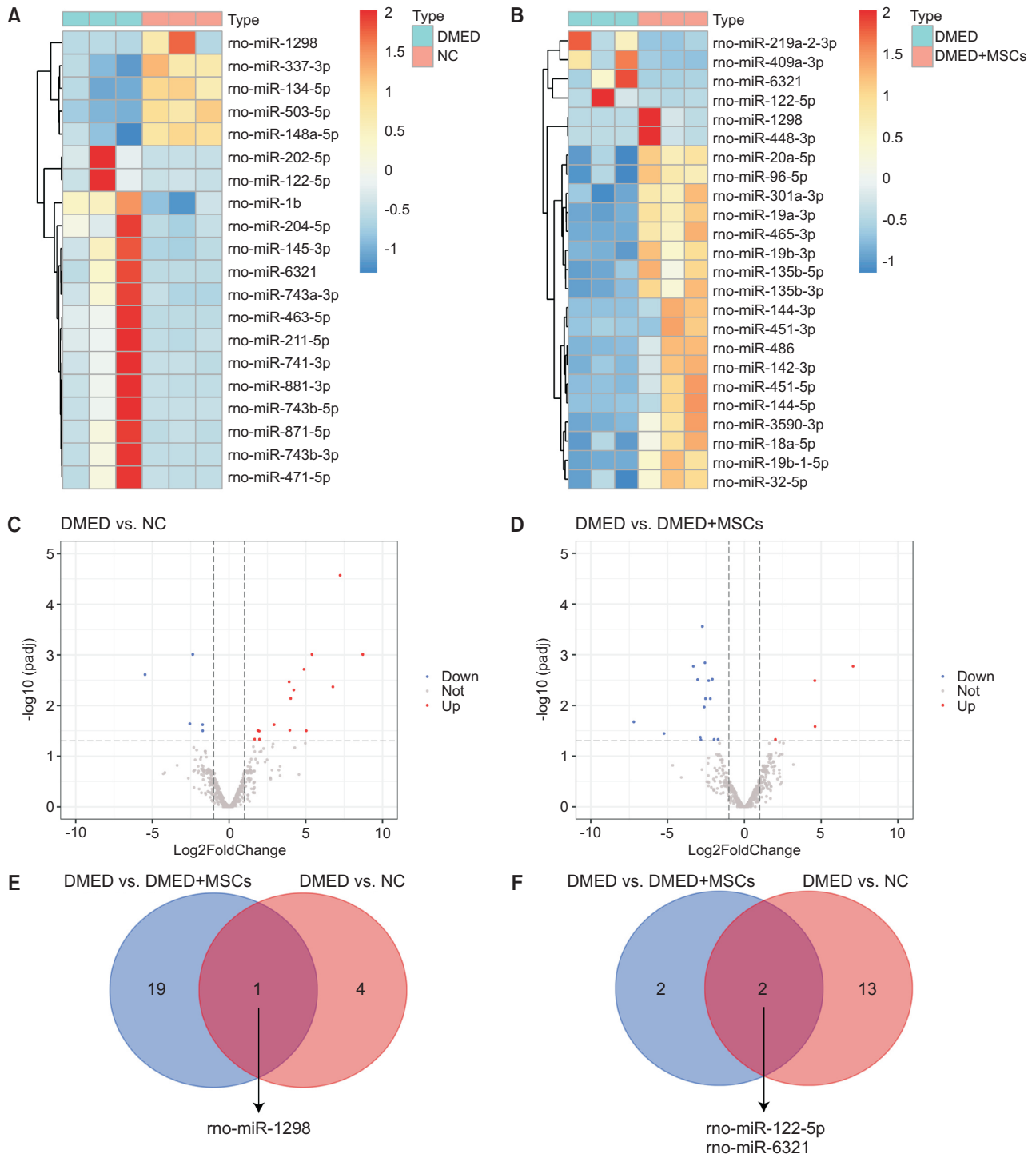


Fig. 3. Identification of DEMs. (A) Heatmap for DMED versus NC. (B) Heatmap for DMED versus DMED+MSCs. (C) Volcano map for DMED versus NC. (D) Volcano map for DMED versus DMED+MSCs. (E) Venn diagram of commonly downregulated DEMs. (F) Venn diagram of commonly up-regulated DEMs. DMED: diabetes mellitus erectile dysfunction, NC: normal control, MSC: mesenchymal stem cell, DEM: differentially expressed miRNA.

factor stimulus (GO:0071363), ossification (GO:0001503), response to steroid hormone (GO:0048545), angiogenesis (GO:0001525), positive regulation of apoptotic process

(GO:0043065) and one Reactome pathway (Innate Immune System) were significantly enriched (Table 4).

Table 2. Key miRNAs in differential expression

miRNA	DMED group vs. NC group		DMED group vs. DMED+MSCs group	
	LogFC	Adjusted p-value	LogFC	Adjusted p-value
rno-miR-1298	-5.480	0.002	-8.877	<0.001
rno-miR-122-5p	4.212	0.005	4.588	0.003
rno-miR-6321	8.715	0.001	7.077	0.002

DMED: diabetes mellitus erectile dysfunction, NC: normal control, MSC: mesenchymal stem cell.

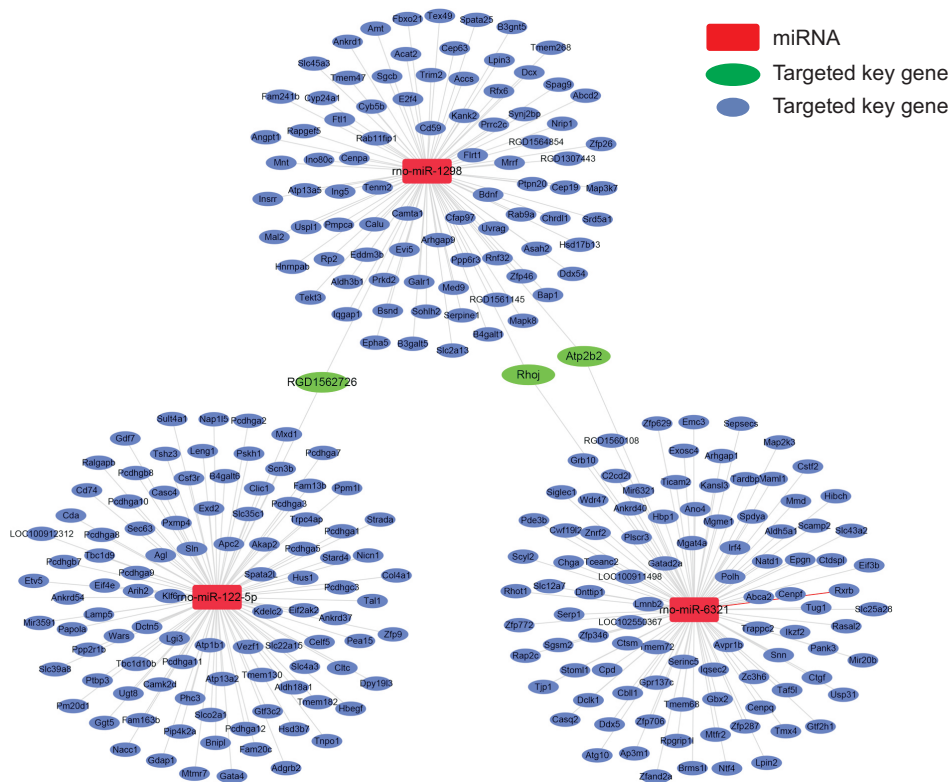


Fig. 4. The network of miRNA-target gene.

6. Validation of hub genes by GEO database

Among the 10 hub genes, we identified 8 genes including Ddx5, Mapk8, B4galt1, Bdnf, Cltc, Map3k7, Ankrd1, and Ctgf in the GSE2457 dataset. As shown in Fig. 8, only the expression of B4galt1 was statistically different ($p < 0.001$). B4galt1 was highly expressed in penile tissues of diabetic rats.

DISCUSSION

Diabetes is regarded as a major risk factor for the onset of ED. However, the complex pathogenesis of DMED, involving multiple factors such as blood vessels, nerves, endocrine, and metabolism, has not been fully elucidated. Therefore, we conducted the study to explore the miRNAs in DMED using high-throughput sequencing and bioinformatic methods. The present

study revealed that rats with DMED showed higher blood glucose but lower bodyweight than the non-diabetic groups, which reflected properly the general pathophysiology of diabetes. The erectile function of rats with DMED was significantly impaired accessed by the ICP experiment but improved after MSC transplantation (Fig. 1). After that, we identified key DEMs and implemented a bioinformatic analysis to screen target genes closely related to DMED and stem cell treatment. We acquired DEMs between DMED *versus* NC group, and DMED *versus* DMED+MSCs group separately, and then got three DEMs overlapped among the two comparisons after taking the intersection. Namely, rno-miR-1298 expressional level was significantly decreased following DMED and upregulated with MSCs treatment. The expression of rno-miR-122-5p and rno-miR-6321 upregulated in DMED increased following

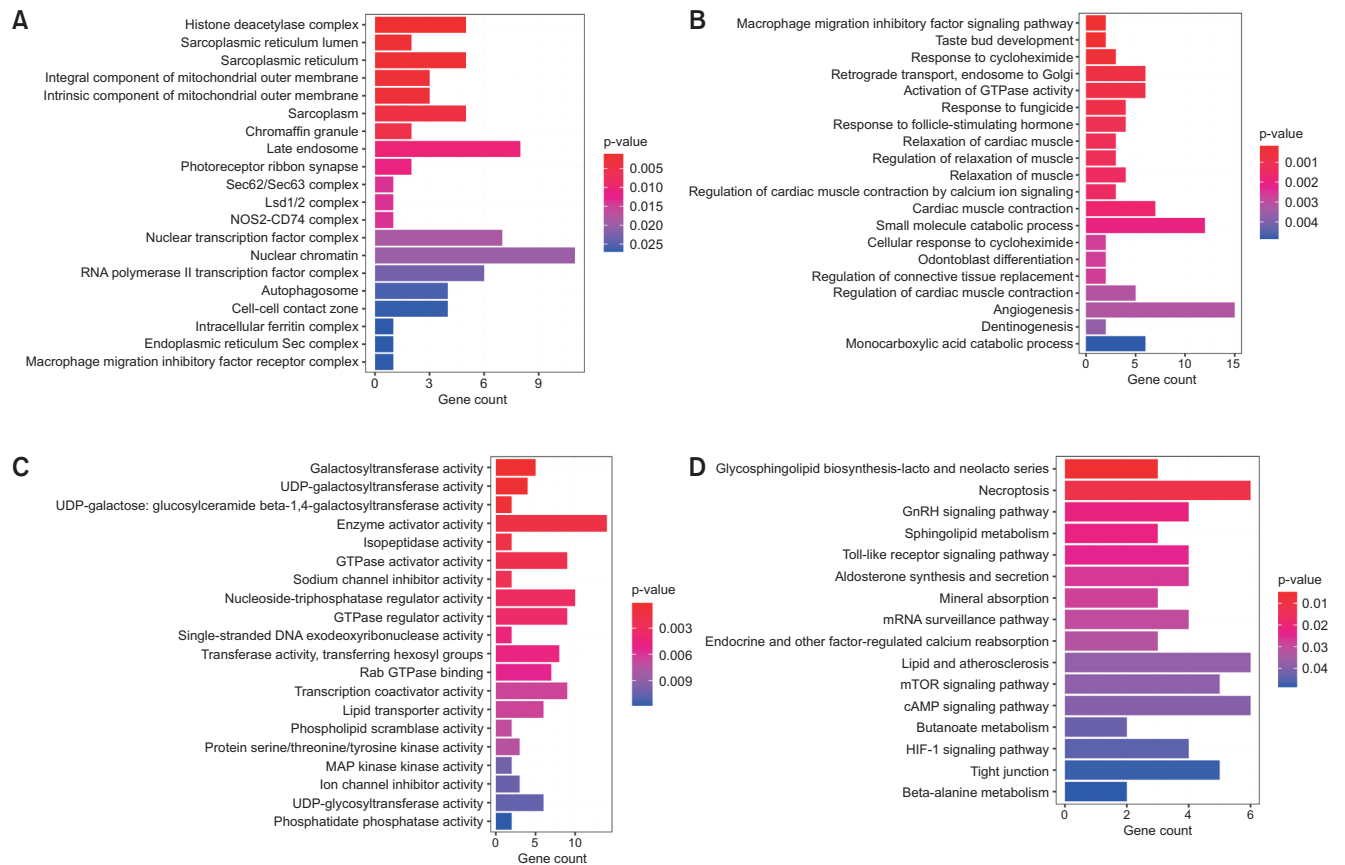


Fig. 5. GO and KEGG enrichment analysis of target genes. (A) Bar plot of top 20 CC terms. (B) Bar plot of top 20 BP terms. (C) Bar plot of top 20 MF terms. (D) Bar plot of significant KEGG pathway terms. GO: Gene Ontology, KEGG: Kyoto Encyclopedia of Genes and Genomes, CC: cellular component, BP: biological process, MF: molecular function.

MSCs intervention. The top 10 target genes including Ddx5, Rhoj, Mapk8, B4galt1, Bdnf, Cltc, Map3k7, Aldh3b1, Ankrd1, and Ctgf were screened according to the degree in the PPI network. Moreover, B4galt1 was equally high expressed in penile tissues of diabetic rats validated by the GSE2457 dataset. As a target gene of rno-miR-1298, B4galt1 would be negatively regulated by rno-miR-1298. Consequently, we speculated that the rno-miR-1298/B4galt1 axis might exert function in stem cell therapy for ED.

In recent years, miRNAs were reported to play roles in ED related to type 2 DM, aging, obesity, and cavernous nerve injury (CNI). Pan reported DEMs in a murine model of DMED for the first time [31]. They found four key DEMs play crucial roles *via* regulating 28 different genes. In particular, miR-18a or miR-206/IGF-1 axis may become novel therapeutic targets for ED treatment. Barbary et al [32] identified miRNAs expressed in corpus cavernosum in a mouse model of diet-induced ED but not explored the function of DEMs.

Similarly, Bai et al [33] studied the miRNA expression of obese rats with ED compared with obese rats without ED. They found 68 DEMs and up-regulation of miR-328a might promote the onset of ED. Pan et al [34] found four upregulated miRNAs including miR-1, miR-200a, miR-203, and miR-206 in the aging-related ED group and they interacted with 13 target genes to regulated PGE1/PKA and eNOS/NO/PKG pathways. Interestingly, miR-1 was also highly expressed in the DMED group in our study. Liu et al [35] detected abnormal miRNA expression in bilateral CNI-induced ED and validated four key miRNAs (miR-101a, miR-138, miR-338, and miR-142) playing roles. Therefore, the roles of miRNAs for ED deserve further exploration.

As is well-known, miRNAs are usually highly conserved so that studying the function of one miRNA in model organisms can help to reverse its function in human diseases. Previous studies emphasized that miR-1298 was often low expressed and served a crucial role of an onco-suppressor gene in several types of cancer,

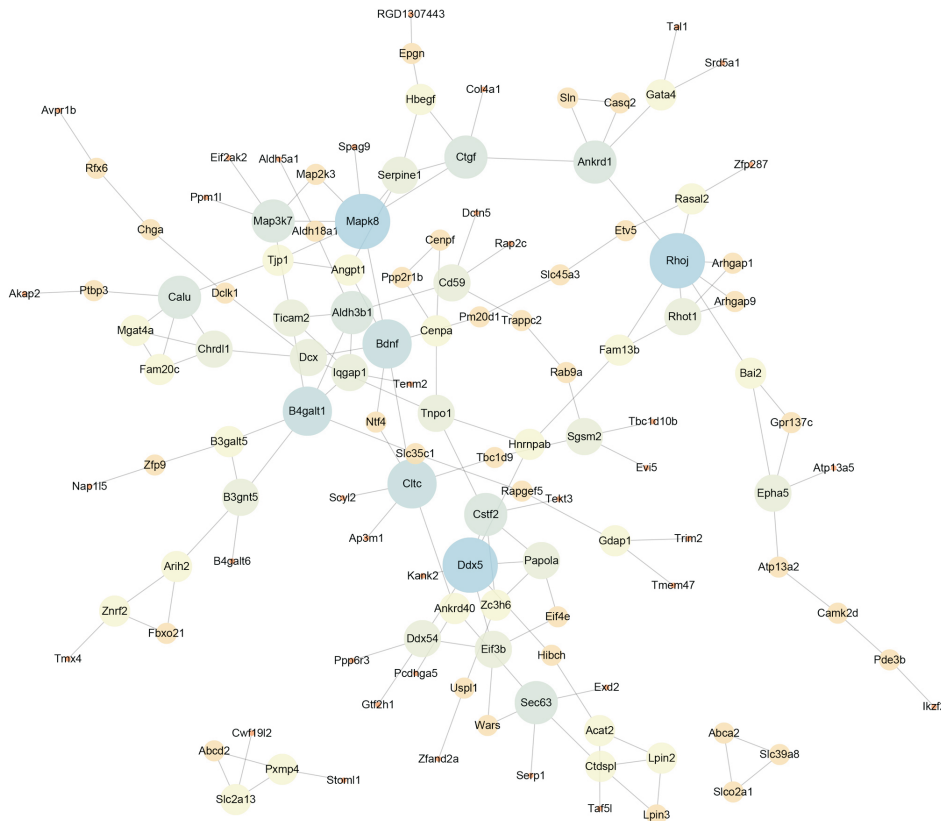


Fig. 6. Protein-protein interaction network of target genes.

including gastric cancer [36], breast cancer [37], cervical cancer [38], and glioma [39]. In addition, Hu et al [40] found that miR-1298 was significantly down-regulated in arteriosclerosis obliterans (ASO) compared with normal arteries. Reduced levels of miR-1298 in atherosclerotic arteries or vascular smooth muscle cells (VSMCs) increased Connexin 43 (Cx43) mRNA levels, unblocked Cx43 translation, and enhanced Cx43 protein levels. Augmented Cx43 expression fosters the switch of VSMC from the contractile to the synthetic state characterized by enhanced proliferation, migration, and neointima formation. Their data demonstrated a specific role of the miR-1298/Cx43 pathway in regulating VSMC function, which provides an idea for studying the mechanism of miR-1298 in DMED.

MiR-122-5p is a particularly interesting miRNA predominantly expressed in the liver, accounting for 70% of total hepatic miRNAs [41]. Previously, the research of miR-122-5p mainly focused on liver diseases, such as liver fibrosis, non-alcoholic steatohepatitis, and hepatocellular carcinoma [42,43]. Moreover, studies showed miR-122 participated in the pathogenesis of arteriosclerosis by regulating epithelial-mesenchymal transition [44,45]. Song et al [46] found that inhibition of miR-122-

5p prevented lipopolysaccharide-induced myocardial injury by inhibiting inflammation, oxidative stress, and apoptosis by targeting GIT1. In the present study, we observed miR-122-5p was increased in the DMED group. The pro-apoptotic effect of miR-122 may help to understand the pathogenesis of DMED.

Recently, the abnormal expression of B4GalT1 has been noted in several human tumors and it is associated with cancer cell proliferation, invasion, migration, and drug resistance. Wang et al's work [47] showed that B4GalT1 expression in glioblastoma tumor tissue was higher than in normal tissue and B4GalT1 knockdown could increase apoptosis and autophagy of glioblastoma *in vitro* and *in vivo*. Zhang et al [13] found autophagy was impaired in DMED rats. According to this, we speculated that B4GalT1, which was highly expressed in DMED, may play a role in regulating autophagy. In addition, De Vitis et al [48] provided the first evidence that B4GalT1 was a stemness factor involving in the maintenance and propagation of lung cancer stem cells, which could become a new potential target of intervention. Furthermore, a latest research by Chen et al [49] suggested that elevated p65 transcriptionally up-regulated B4GALT1 expression to

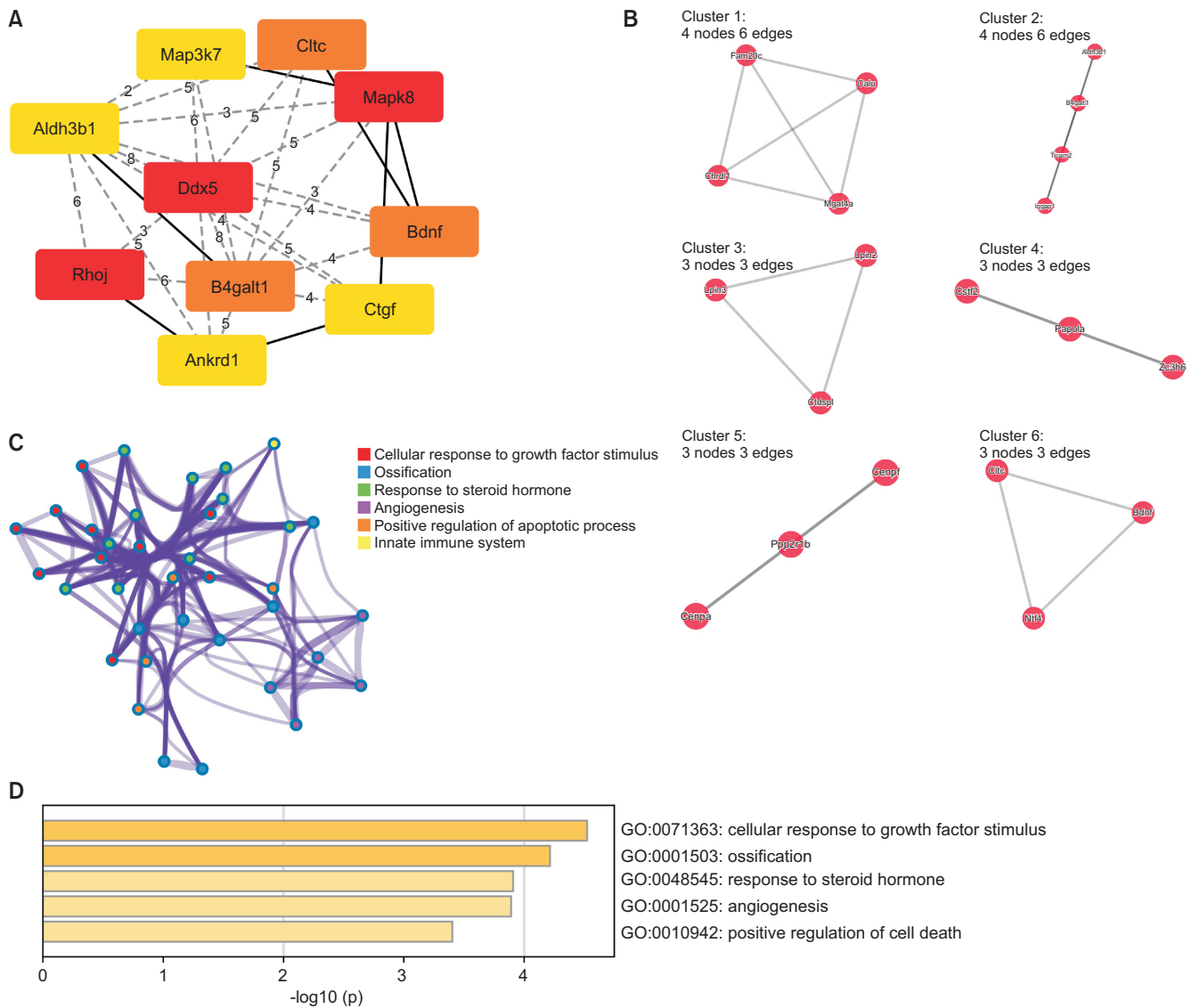


Fig. 7. Identification of hub genes from PPI and functional enrichment analysis through Metascape. (A) Ten hub genes identified by cytoHubba. (B) Six key clusters detected by MCODE. (C) The network of enrichment analysis across 10 hub genes, where nodes that share the same pathway are typically close to each other. (D) Bar plot of enrichment analysis across 10 hub genes, colored by p-values.

Table 3. The basic information of 10 hub genes with the highest degrees by CytoHubba

Name	Full name	Ensembl ID	Degree
Ddx5	DEAD-box helicase 5	ENSRNOG00000030680	7
Rhoj	Ras homolog family member	ENSRNOG00000021919	7
Mapk8	Mitogen-activated protein kinase 8	ENSRNOG00000020155	7
B4galt1	Beta-1,4-galactosyltransferase 1	ENSRNOG00000059461	6
Bdnf	Brain-derived neurotrophic factor	ENSRNOG00000047466	6
Cltc	Clathrin heavy chain	ENSRNOG00000004291	6
Map3k7	Mitogen activated protein kinase kinase kinase 7	ENSRNOG00000005724	5
Aldh3b1	Aldehyde dehydrogenase 3 family, member B1	ENSRNOG00000017512	5
Ankrd1	Ankyrin repeat domain 1	ENSRNOG00000018598	5
Ctgf	Cellular communication network factor 2	ENSRNOG00000015036	5

Table 4. Functional enrichment analysis of 10 hub genes through Metascape

Category	ID	Description	p-value	Count	Symbols
GO biological processes	GO:0071363	Cellular response to growth factor stimulus	2.67E-05	5	Bdnf, Ankrd1, Ccn2, Ddx5, Map3k7, Mapk8
GO biological processes	GO:0001503	Ossification	5.66E-05	4	Ccn2, Mapk8, Ddx5, Map3k7, Rhoj, Cltc
GO biological processes	GO:0048545	Response to steroid hormone	1.13E-04	4	Bdnf, Ccn2, Mapk8, Ddx5, Map3k7, B4galt1
GO biological processes	GO:0001525	Angiogenesis	1.16E-04	4	B4galt1, Ccn2, Rhoj, Map3k7
GO biological processes	GO:0043065	Positive regulation of apoptotic process	3.08E-04	4	B4galt1, Ankrd1, Ccn2, Mapk8, Map3k7
Reactome gene sets	R-RNO-168249	Innate Immune System	4.93E-04	4	B4galt1, Mapk8, Aldh3b1, Map3k7

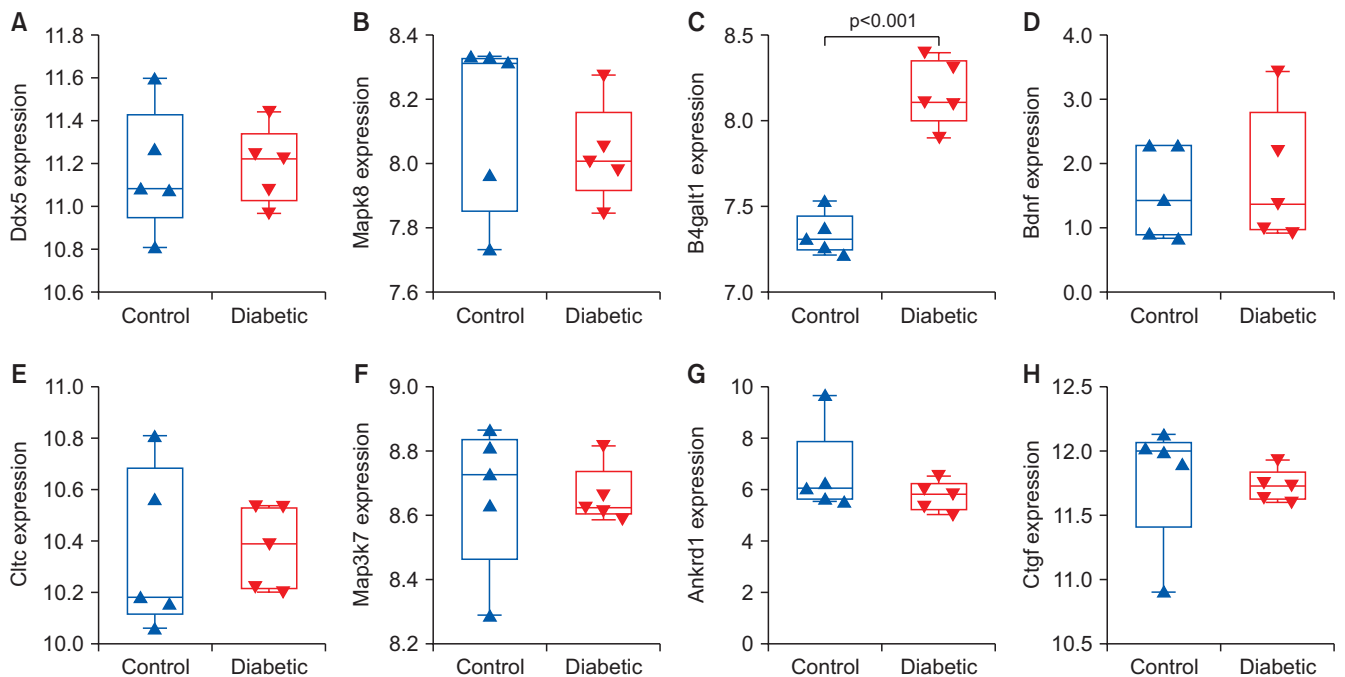


Fig. 8. The mRNA expression of hub genes was determined from the GSE2457 dataset. (A) Ddx5. (B) Mapk8. (C) B4galt1. (D) Bdnf. (E) Cltc. (F) Map3k7. (G) Ankrd1. (H) Ctgf.

enhance the N-linked glycosylation of CDK11, which in turn modulated cancer chemoresistance and cancer progression. Consequently, the roles B4GalT1 plays in DMED are deserved to study.

Although increasing evidence suggests that stem cell transplantation showed an effective contribution to the improvement of DMED, its mechanism has not been established clearly. Exosomes derived from MSCs were suggested to be beneficial to erectile function in DM rats [50]. Huo et al [51] found MSCs-derived exosomal miRNA-21-5p enhanced proliferation and reduced apoptosis of corpus cavernosum smooth muscle cells *via* downregulating PDCD4 to ameliorate ED in a rat model of DM. In this study, we also proved the positive effect of stem cells on DMED. In addition, we analyzed

the miRNA expression profile of the corpus cavernosum after stem cell therapy, trying to help explore the mechanism of stem cell action, but this still requires further experiments.

Indeed, several limitations of our study should be addressed. Firstly, our experiments were conducted in normal animals, which cannot completely imitate the pathological changes of *in vivo* conditions. Secondly, we focused on miRNAs between DMED and normal rats at a certain time. However, some of these may vary during the progression of DMED, which results in missing crucial information. Thirdly, the miRNA-gene interaction was predicted through public databases, and the regulatory relationship should be validated by further experiments.

CONCLUSIONS

Taken together, our study analyzed the miRNA expression profile in DMED rats with stem cell therapy for the first time. Of them, three key miRNAs (rno-miR-1298, rno-miR-122-5p, and rno-miR-6321) were significantly dysregulated. In addition, based on the negative regulatory relationship, the miR-1298/B4GalT1 axis might exert function in stem cell therapy for ED. Further functional experimentation is needed to confirm these findings.

Conflict of Interest

The authors have nothing to disclose.

Funding

This research was supported by Zhao Yi-Cheng Medical Science Foundation (ZYYFY2018031).

Authors Contributions

Conceptualization: JK, YS, XL. Data curation: JK, YS, ZZ, SW. Formal analysis: JK, YS, YL. Methodology: JK, YS. Software: JK, YL. Supervision: XL. Writing – original draft: JK. Writing – review & editing: all authors.

Data Sharing Statement

The data that support the findings of this study cannot be publicized, but are available from the corresponding author upon reasonable request.

REFERENCES

1. NIH Consensus Conference. Impotence. NIH consensus development panel on impotence. *JAMA* 1993;270:83-90.
2. Najari BB, Kashanian JA. Erectile dysfunction. *JAMA* 2016;316:1838.
3. Salonia A, Castagna G, Saccà A, Ferrari M, Capitanio U, Castiglione F, et al. Is erectile dysfunction a reliable proxy of general male health status? The case for the International Index of Erectile Function-Erectile Function domain. *J Sex Med* 2012;9:2708-15.
4. Capogrosso P, Ventimiglia E, Boeri L, Capitanio U, Gandaglia G, Dehò F, et al. Sexual functioning mirrors overall men's health status, even irrespective of cardiovascular risk factors. *Andrology* 2017;5:63-9.
5. Kouidrat Y, Pizzol D, Cosco T, Thompson T, Carnaghi M, Bertoldo A, et al. High prevalence of erectile dysfunction in diabetes: a systematic review and meta-analysis of 145 studies. *Diabet Med* 2017;34:1185-92.
6. Castela Â, Costa C. Molecular mechanisms associated with diabetic endothelial-erectile dysfunction. *Nat Rev Urol* 2016;13:266-74.
7. Hatzichristou D, d'Anzeo G, Porst H, Buvat J, Henneges C, Rossi A, et al. Tadalafil 5 mg once daily for the treatment of erectile dysfunction during a 6-month observational study (EDATE): impact of patient characteristics and comorbidities. *BMC Urol* 2015;15:111.
8. Gur S, Abdel-Mageed AB, Sikka SC, Hellstrom WJG. Advances in stem cell therapy for erectile dysfunction. *Expert Opin Biol Ther* 2018;18:1137-50.
9. Zhou F, Hui Y, Xin H, Xu YD, Lei HE, Yang BC, et al. Therapeutic effects of adipose-derived stem cells-based microtissues on erectile dysfunction in streptozotocin-induced diabetic rats. *Asian J Androl* 2017;19:91-7.
10. Jeon SH, Zhu GQ, Bae WJ, Choi SW, Jeong HC, Cho HJ, et al. Engineered mesenchymal stem cells expressing stromal cell-derived factor-1 improve erectile dysfunction in streptozotocin-induced diabetic rats. *Int J Mol Sci* 2018;19:3730.
11. Sun X, Luo LH, Feng L, Li DS. Down-regulation of lncRNA MEG3 promotes endothelial differentiation of bone marrow derived mesenchymal stem cells in repairing erectile dysfunction. *Life Sci* 2018;208:246-52.
12. Kwon MH, Song KM, Limanjaya A, Choi MJ, Ghatak K, Nguyen NM, et al. Embryonic stem cell-derived extracellular vesicle-mimetic nanovesicles rescue erectile function by enhancing penile neurovascular regeneration in the streptozotocin-induced diabetic mouse. *Sci Rep* 2019;9:20072.
13. Zhang C, Luo D, Li T, Yang Q, Xie Y, Chen H, et al. Transplantation of human urine-derived stem cells ameliorates erectile function and cavernosal endothelial function by promoting autophagy of corpus cavernosal endothelial cells in diabetic erectile dysfunction rats. *Stem Cells Int* 2019;2019:2168709.
14. Teo AK, Vallier L. Emerging use of stem cells in regenerative medicine. *Biochem J* 2010;428:11-23.
15. Chen Z, Han X, Ouyang X, Fang J, Huang X, Wei H. Transplantation of induced pluripotent stem cell-derived mesenchymal stem cells improved erectile dysfunction induced by cavernous nerve injury. *Theranostics* 2019;9:6354-68.
16. Liu Q, Cui Y, Lin H, Hu D, Qi T, Wang B, et al. MicroRNA-145 engineered bone marrow-derived mesenchymal stem cells alleviated erectile dysfunction in aged rats. *Stem Cell Res Ther* 2019;10:398.

17. Lee RC, Feinbaum RL, Ambros V. The *C. elegans* heterochronic gene *lin-4* encodes small RNAs with antisense complementarity to *lin-14*. *Cell* 1993;75:843-54.
18. Wang J, Chen J, Sen S. MicroRNA as biomarkers and diagnostics. *J Cell Physiol* 2016;231:25-30.
19. Chen S, Sun X, Wu S, Jiang J, Zhu C, Xu K, et al. Role of identified noncoding RNA in erectile dysfunction. *Andrologia* 2020;52:e13596.
20. Wen Y, Liu G, Zhang Y, Li H. MicroRNA-205 is associated with diabetes mellitus-induced erectile dysfunction via down-regulating the androgen receptor. *J Cell Mol Med* 2019;23:3257-70.
21. Heaton JP, Varrin SJ, Morales A. The characterization of a bio-assay of erectile function in a rat model. *J Urol* 1991;145:1099-102.
22. Gholami SS, Rogers R, Chang J, Ho HC, Grazziottin T, Lin CS, et al. The effect of vascular endothelial growth factor and adeno-associated virus mediated brain derived neurotrophic factor on neurogenic and vasculogenic erectile dysfunction induced by hyperlipidemia. *J Urol* 2003;169:1577-81.
23. Robinson MD, McCarthy DJ, Smyth GK. edgeR: a bioconductor package for differential expression analysis of digital gene expression data. *Bioinformatics* 2010;26:139-40.
24. Krüger J, Rehmsmeier M. RNAhybrid: microRNA target prediction easy, fast and flexible. *Nucleic Acids Res* 2006;34:W451-4.
25. John B, Enright AJ, Aravin A, Tuschl T, Sander C, Marks DS. Human MicroRNA targets. *PLoS Biol* 2004;2:e363.
26. Shannon P, Markiel A, Ozier O, Baliga NS, Wang JT, Ramage D, et al. Cytoscape: a software environment for integrated models of biomolecular interaction networks. *Genome Res* 2003;13:2498-504.
27. Szklarczyk D, Morris JH, Cook H, Kuhn M, Wyder S, Simonovic M, et al. The STRING database in 2017: quality-controlled protein-protein association networks, made broadly accessible. *Nucleic Acids Res* 2017;45:D362-8.
28. Yu G, Wang LG, Han Y, He QY. clusterProfiler: an R package for comparing biological themes among gene clusters. *OMICS* 2012;16:284-7.
29. Zhou Y, Zhou B, Pache L, Chang M, Khodabakhshi AH, Tanaseichuk O, et al. Metascape provides a biologist-oriented resource for the analysis of systems-level datasets. *Nat Commun* 2019;10:1523.
30. Sullivan CJ, Teal TH, Luttrell IP, Tran KB, Peters MA, Wessells H. Microarray analysis reveals novel gene expression changes associated with erectile dysfunction in diabetic rats. *Physiol Genomics* 2005;23:192-205.
31. Pan F, You J, Liu Y, Qiu X, Yu W, Ma J, et al. Differentially expressed microRNAs in the corpus cavernosum from a murine model with type 2 diabetes mellitus-associated erectile dysfunction. *Mol Genet Genomics* 2016;291:2215-24.
32. Barbery CE, Celigoj FA, Turner SD, Smith RP, Kavoussi PK, Annex BH, et al. Alterations in microRNA expression in a murine model of diet-induced vasculogenic erectile dysfunction. *J Sex Med* 2015;12:621-30.
33. Bai Y, Zhang L, Jiang Y, Ju J, Li G, Xu J, et al. Identification and functional verification of MicroRNAs in the obese rat with erectile dysfunction. *Sex Med* 2017;5:e261-71.
34. Pan F, Xu J, Zhang Q, Qiu X, Yu W, Xia J, et al. Identification and characterization of the MicroRNA profile in aging rats with erectile dysfunction. *J Sex Med* 2014;11:1646-56.
35. Liu C, Cao Y, Ko TC, Chen M, Zhou X, Wang R. The changes of MicroRNA expression in the corpus cavernosum of a rat model with cavernous nerve injury. *J Sex Med* 2018;15:958-65.
36. Qiu ZK, Liu N, Zhao SF, Ding AP, Cheng G, Qiu WS, et al. MiR-1298 expression correlates with prognosis and inhibits cell proliferation and invasion of gastric cancer. *Eur Rev Med Pharmacol Sci* 2018;22:1672-9.
37. Zhang J, Hu D. miR-1298-5p influences the malignancy phenotypes of breast cancer cells by inhibiting CXCL11. *Cancer Manag Res* 2021;13:133-45.
38. Zhang H, Zhang R, Zhang G, Liu W, Ma Z, Yue C, et al. Clinical significance of miR-1298 in cervical cancer and its biological function in vitro. *Oncol Lett* 2021;21:401.
39. Xu X, Ban Y, Zhao Z, Pan Q, Zou J. MicroRNA-1298-3p inhibits proliferation and invasion of glioma cells by downregulating Nidogen-1. *Aging (Albany NY)* 2020;12:7761-73.
40. Hu W, Wang M, Yin H, Yao C, He Q, Yin L, et al. MicroRNA-1298 is regulated by DNA methylation and affects vascular smooth muscle cell function by targeting connexin 43. *Cardiovasc Res* 2015;107:534-45.
41. Chang J, Nicolas E, Marks D, Sander C, Lerro A, Buendia MA, et al. miR-122, a mammalian liver-specific microRNA, is processed from hcr mRNA and may downregulate the high affinity cationic amino acid transporter CAT-1. *RNA Biol* 2004;1:106-13.
42. Bandiera S, Pfeffer S, Baumert TF, Zeisel MB. miR-122--a key factor and therapeutic target in liver disease. *J Hepatol* 2015;62:448-57.
43. Yin S, Fan Y, Zhang H, Zhao Z, Hao Y, Li J, et al. Differential TGFβ pathway targeting by miR-122 in humans and mice affects liver cancer metastasis. *Nat Commun* 2016;7:11012.
44. Wu X, Du X, Yang Y, Liu X, Liu X, Zhang N, et al. Inhibition of miR-122 reduced atherosclerotic lesion formation by regulating NPAS3-mediated endothelial to mesenchymal transi-

- tion. *Life Sci* 2021;265:118816.
45. Li Y, Yang N, Dong B, Yang J, Kou L, Qin Q. MicroRNA-122 promotes endothelial cell apoptosis by targeting XIAP: therapeutic implication for atherosclerosis. *Life Sci* 2019;232:116590.
 46. Song W, Zhang T, Yang N, Zhang T, Wen R, Liu C. Inhibition of micro RNA miR-122-5p prevents lipopolysaccharide-induced myocardial injury by inhibiting oxidative stress, inflammation and apoptosis via targeting GIT1. *Bioengineered* 2021;12:1902-15.
 47. Wang P, Li X, Xie Y. B4GalT1 regulates apoptosis and autophagy of glioblastoma in vitro and in vivo. *Technol Cancer Res Treat* 2020;19:1533033820980104.
 48. De Vitis C, Corleone G, Salvati V, Ascenzi F, Pallocca M, De Nicola F, et al. B4GALT1 is a new candidate to maintain the stemness of lung cancer stem cells. *J Clin Med* 2019;8:1928.
 49. Chen Y, Su L, Huang C, Wu S, Qiu X, Zhao X, et al. Galactosyltransferase B4GALT1 confers chemoresistance in pancreatic ductal adenocarcinomas by upregulating N-linked glycosylation of CDK11p110. *Cancer Lett* 2021;500:228-43.
 50. Zhu LL, Huang X, Yu W, Chen H, Chen Y, Dai YT. Transplantation of adipose tissue-derived stem cell-derived exosomes ameliorates erectile function in diabetic rats. *Andrologia* 2018;50:e12871.
 51. Huo W, Li Y, Zhang Y, Li H. Mesenchymal stem cells-derived exosomal microRNA-21-5p downregulates PDCD4 and ameliorates erectile dysfunction in a rat model of diabetes mellitus. *FASEB J* 2020;34:13345-60.